

ПОРОШКОВАЯ МЕТАЛЛУРГИЯ И КОМПОЗИЦИОННЫЕ МАТЕРИАЛЫ

УДК 620.17

МЕТАЛЛОКОМПОЗИТНОЕ СОЕДИНЕНИЕ И ЕГО МЕХАНИЧЕСКИЕ ХАРАКТЕРИСТИКИ

Лю Лунцюань, Ши Цзяньхан, Бао Хайшен

*Институт авиации и космонавтики, Шанхайский университет
Цзяо Тонг, Шанхай, 200240, Китай*

Статья поступила в редакцию 03.06.2019

Предложен прикладной метод, который может быть использован для повышения прочности металлокомпозитных соединений.

В таком виде соединений будет определенное количество тонких штифтов, проходящих через подложки в области перекрытия металлокомпозитных клеевых соединений. На поверхности штифтов имеется клей, и таким образом штифты соединяются с подложками.

Штифты, проходящие через соединительные пластины, не только устраняют трещины в адгезивном слое связанных соединений, но и воспринимают некоторую нагрузку между металлическими и композитными компонентами.

Результаты испытаний показывают, что предложенный метод может увеличить прочность и устойчивость к разрушению металлокомпозитных соединений по сравнению с традиционными клеевыми соединениями.

Влияние количества и расположения штифтов на механические характеристики соединения проанализировано в соответствии с результатами испытаний.

И наконец, получен метод оптимизации, применение которого позволит улучшить показатели по нагрузочной способности и изломостойкости соединений.

Ключевые слова: металлокомпозитное соединение, композиционные материалы, конечно-элементная модель, механические характеристики, металлический штифт.

Библиографический список

1. Zimmermann K., Zenkert D., Siemetzki M. Testing and analysis of ultra thick composites // Composites Part B: Engineering. 2010. Vol. 41. No. 4, pp. 326-336. DOI: 10.1016/j.compositesb.2009.12.004

2. Wu F.Q., Yao W.X. A model of the fatigue life distribution of composite laminates based on their static strength distribution // Chinese Journal of Aeronautics. 2008. Vol. 21. No. 3, pp. 241-246. DOI: 10.1016/S1000-9361(08)60031-X

3. Löbel T., Holztüter D., Sinapius M., Hühne C. A hybrid bondline concept for bonded composite joints // International Journal of Adhesion and Adhesives. 2016. Vol. 68, pp. 229-238. DOI: 10.1016/j.ijadhadh.2016.03.025
4. Yoon T.H., Kim S.J. Refined numerical simulation of three-dimensional riveting in laminated composites // Journal of Aircraft. 2011. Vol. 48. No. 4, pp. 1434-1443. DOI: 10.2514/1.C031311
5. Restivo G., Marannano G., Isaicu G.A. Three-dimensional strain analysis of single-lap bolted joints in thick composites using fibre-optic gauges and the finite-element method // The Journal of Strain Analysis for Engineering Design. 2010. Vol. 45. No. 7, pp. 523-534. DOI: 10.1243/03093247JSA599
6. Sen F., Pakdil M., Sayman O., Benli S. Experimental failure analysis of mechanically fastened joints with clearance in composite laminates under preload // Materials & Design. 2008. Vol. 29. No. 6, pp. 1159-1169.
7. Budhe S., Banea M.D., de Barros S., da Silva L.F.M. An updated review of adhesively bonded joints in composite materials // International Journal of Adhesion and Adhesives. 2017. Vol. 72, pp. 30-42. DOI: 10.1016/j.ijadhadh.2016.10.010
8. Advisory circular 20-107B subject: composite aircraft structure U.S. -Department of Transportation – Federal Aviation Administration (FAA), 2010.
9. AMC 20-29 Annex II to ED Decision 2010/003/R of 19.07.2010. - European Aviation Safety Agency (EASA), 2009.
10. Richard L., Lin K.Y. Analytical and Experimental Studies on Delamination Arrest in Bolted-Bonded Composite Structures // 58th AIAA/ASCE/AHS/ASC Structures, Structural Dynamics, and Materials Conference. 9 - 13 January 2017, Grapevine, Texas, 12 p. DOI: 10.2514/6.2016-1502
11. Richard L.I., Liu W., Lin K.Y. Delamination Arrest by Multiple Fasteners in Bonded Composite Structures // 55th AIAA/ASME/ASCE/AHS/ASC Structures, Structural Dynamics, and Materials Conference, National Harbor, Maryland, 2014, 10 p.
12. Action J.E., Engelstad S.P. Crack Arrestment of Pi-Joined Bonded Composites // 55th AIAA/ASME/ASCE/AHS/ASC Structures, Structural Dynamics, and Materials Conference, National Harbor, Maryland, 2014, 17 p.
13. Huang J., Rapoff A. J., Hafika R.T. Arresting cracks in bone-like composites // 44th AIAA/ASME/ASCE/AHS Structures, Structural Dynamics, and Materials Conference, Virginia, 2003, 11 p.
14. Kruse T., Körwien T., Heckner S., Geistbeck M. Bonding of CFRP primary aerospace structures—crackstopping in composite bonded joints under fatigue // Proceedings of the 20th International Conference on Composite Materials (ICCM/20), Copenhagen, 19-24th July 2015, pp. 795-808.
15. Sachse R., Picket A.K., Käß M., Middendorf P. Numerical simulation of fatigue crack growth in the adhesive bondline of hybrid CFRP joints // Proceedings of the conference on the mechanical response of composites (ECCOMAS), Bristol, 2015.
16. Freeman R., Smith F. Comeld: a novel method of composite to metal joining // Advanced Material Process. 2005. Vol. 163. No. 4, pp. 33-40.

A METAL-COMPOSITE JOINT AND ITS MECHANICAL PERFORMANCE

Liu Longquan, Shi Jianhang, Bao Haisheng

*School of Aeronautics and Astronautics, Shanghai Jiao Tong University,
Shanghai, China*

A jointing technique, which can be employed in metal-composite joints and may enhance the ability to non-admission of joints disbond, is proposed in this article. This type of joints will contain a certain number of thin pins running through the substrates in the overlap region of the metal-composite adhesive bonded joints. There is adhesive on the surface of the pins and thus, the pins are bonded together with the substrates. And thus, the pins running through the joint plates not only arrest the cracks in the adhesive layer of the bonded joints, also transfer some load between the metallic and composite components. Comparative test results show that the proposed joint method can increase the strength, the failure strain of the metal-composite joints comparing with the traditional adhesive joints, moreover, the joint method can decrease the suddenness of the joint significantly and therefore, improve the damage tolerance performance of the bonded joints. Secondly, the effects of the number and arrangement of the pins on the mechanical performance of the joint will be analyzed in accordance to the test results also. And finally, an optimized method which can improve the load capacity and fracture toughness of the joints will be obtained.

Keywords: metal-composite joint, composite materials, finite element models, mechanical performance, metallic pins

1. Introduction

Composite materials are increasingly utilized in aviation structures due to their comparatively high specific strength and stiffness and the potentiality of reducing energy consumption [1, 2]. Although the application of composite materials increases the integrity of aircraft structures, many composite components still need be connected together with metallic components to optimize the strength, weight and durability of structures by combining traditional metals with composite materials. For instance, composites are structurally more efficient than metals, but metals have better damage tolerance and failure predictability than composites and are unaffected by solvents and temperature which tend to degrade polymers [3]. Therefore, in order to optimize the benefits provided by both types of materials, multi-material joints between metals and composite materials are increasingly being developed. Traditionally, there are two common used methods to connect the composite and metallic components: mechanical fastening and adhesive bonding. Among these methods, fastening joint is relatively more reliable to transfer higher loads, easier to assemble and disassemble, more tolerant to environmental damages, and helpful in preventing interlamination [4–5]. However, the enhanced stress concentration around the fastener hole often decreases the load carrying capacity of the composite structures [6].

Adhesive bonding has higher load transfer efficiency comparing with fastening joints. Nevertheless, the failure of adhesively bonded joints

often fails tragically without any signs due to the brittle nature of the adhesive layer and the high stress concentration at the ends of adhesive joints [7]. This makes the adhesive bonding is difficult to meet the damage tolerance requirements of transport category airplanes (FAR 25.571) and cannot used in the primary loading structures of the aircrafts up to now. Despite a rigorous manufacturing quality management, one of the following methods has to be established to attain certification [8, 9]: 1) Disbond greater than a pre-defined maximum must be prevented by design features. The allowed disbond maximum must be determined by analysis, test, or both.; 2) Proof testing has to be executed for every production article to ensure that the joint can withstand the desired design loads; 3) The load-bearing capability of each joint must be determined by repeatable and reliable non-destructive inspection (NDI) methods.

To improve the damage tolerance performance of the adhesive joints, many disbond-stopping (crack-arresting) technologies were developed or under investigation to limit the maximum disbond size in adhesively bonded joints as a mean of comply to airworthiness requirements, such as bonded-bolted [10–12], soft inclusions [13], surface and geometry modification [14], rivetless nut plates [15], Comeld [16], hybrid Adhesive bondline architecture [2], etc. However, most of those technologies are not suitable to be applied to the metal-composite hybrid joints due to the differences of the manufacturing process and physical properties between metallic and composite materials.

In this paper, a joint method, which can be used in metal-composite joints and can increase the disbond-stopping abilities of the joints, will be developed and its structural performance discussed in detail.

2. Metal-composite joint specimens

In accordance with this design concept, some metal-composite joints are design and manufactured, as shown in Fig. 1. The dimensions of the specimens were reference to the American Society for Testing and Materials ASTM D 1002. Dimensions of the both plates are 100 mm × 25 mm × 2 mm in length, width and thickness. The length of the bonding zone is 12.7 mm and the thickness is about 0.1 mm. There are 15 pins (3 rows and 5 columns) running through the joint plates in the faying zong. The row distance is 3 mm and column distance is 5 mm. The diameter of the pins is 0.8 mm.

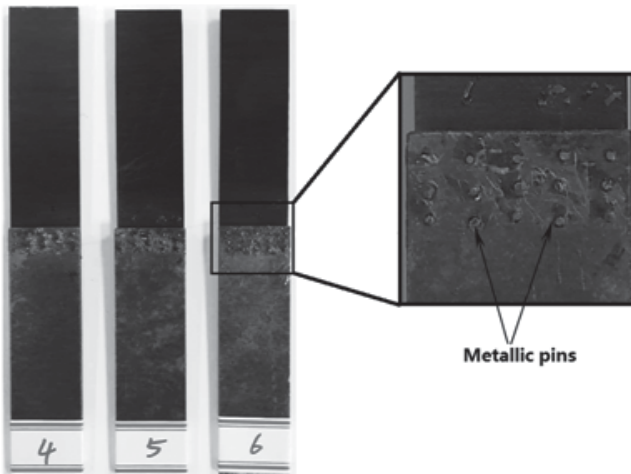


Fig. 1. Metal-composite single lap joints

The composite plate is made of carbon fiber/epoxy composite laminate with 0.188 mm nominal ply thickness and the laminate's stacking sequence is $[\pm 45/0/90]_{2s}$. The materials of the metallic plate and pins are both 45# steel (similar to AISI 1045). The adhesive used to bond the metallic pin with the joint plates is HY-914 and that between the two adherents is Hysol EA9696. Their mechanical properties are listed in Table 2 and Table 3, respectively.

Three specimens with the same geometry features but without the pin were also manufactured for comparison.

3. Experimental studies

Both the two different types of the specimens were tensile tested on a universal testing machine of type MTS CMT 5105 in accordance with ASTM D 1002-10 standard [16]. The test setup is shown in Fig. 2. The

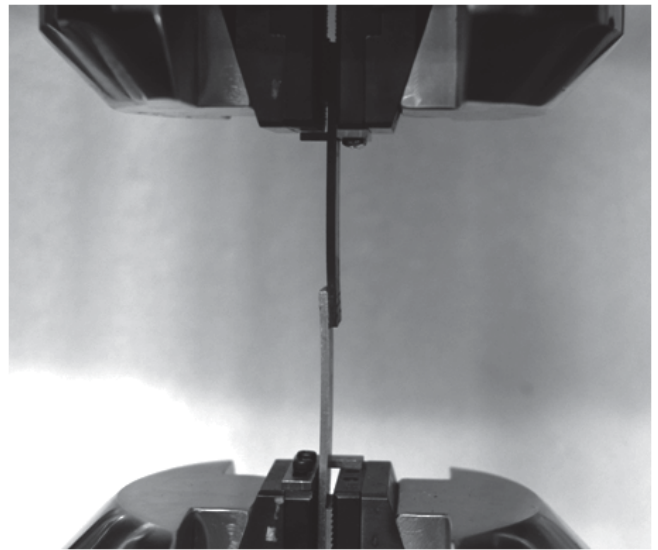


Fig. 2. Tensile test setup

specimens were clamped in the grips of the testing machine and outer 25 mm of each end were in contact with the jaws. Pads with the same thickness of the joined plates were attached at both ends of the samples to make the longitude axis of the test samples to be coincided with the direction of applied load. The load was displacement-controlled with a free crosshead velocity of 0.2 mm/min. The load and displacement were recorded using the embedded transducers with a sampling frequency of 5 Hz.

A typical experimental results is shown in Fig. 3. The load vs displacement curves demonstrate that proposed joints have a significantly greater load carrying capability and failure strain than adhesive joints. The area under the load–displacement curves represents the energy absorbed during failure of the specimens. For both types of joints, the energy

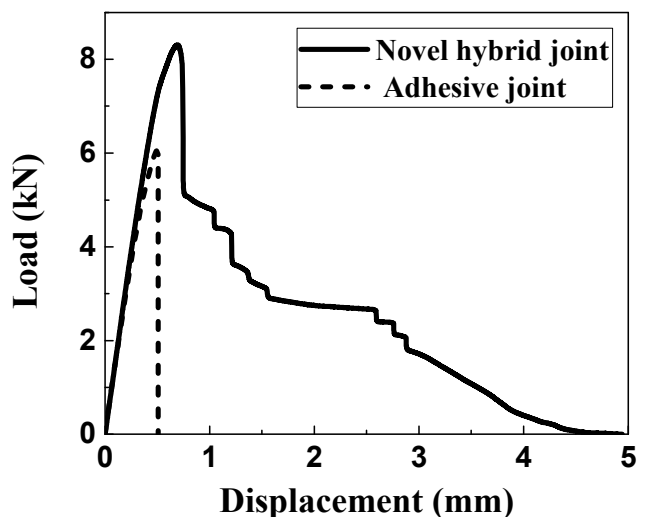


Fig. 3. Load-displacement curves of the metal-composite joints

absorbed by proposed joint is more than four times that absorbed by the traditional adhesive joint. Moreover, adhesive joint fails at the bond line very suddenly and dramatically, as indicated by the sharp change in slope of the corresponding curves.

The two types of joints have different failure mode, as shown in Fig. 4. Adhesive joint is damaged under the action of the shearing force and adhesion between the metal plate and the composite plate takes place cohesive destruction. There was very little damage to the metal or composite parts. As for adhesive-multi pin joint, adhesion did not fail at low loads, the composite material occurred damage when loads reached its failure strength. Damage was visible before failure caused by matrix cracking, whereas adhesive occurred failure abruptly. The composite material is destroyed in the direction of 45° layer. It also can be seen that

the angle of some metal pins change significantly before and after joint breaking. Some metal pins occurred plastic deformation and evenly occurred fracture failure. The adhesive-multi pin joint eventually failed due to fracture failure of metal pins and shear failure of the composite, which contributed to different mechanical behaviors. Therefore, it can be considered that the improvement of mechanical behaviors between the composite part and the metal part mainly because pin not only inhibits the peeling of the adhesive layer, but also pass the load between the connected parts together with the adhesive layer.

4. Numerical simulation

4.1. Meshes and boundary conditions

Finite element models of the joints under tensile loading were developed using Abaqus software, as schematically illustrated in Fig. 5. The finite element model of the joint includes solid models of metallic and composite plates (modelled as C3D8R element in ABAQUS). Composite laminate is modelled with four elements in thickness direction, and each element represents four laminate plies. The adhesive layer on the faying surface of the joint plates was modeled as 8-node cohesive elements (COH3D8) with a 0.1 mm thickness.

The symmetric surfaces of the two joint plates are constrained in translational direction U_y . The left end of steel plate is fixed in all three translational directions (U_x , U_y and U_z). The right end of the laminate plate is declared as a rigid body and has tie relationship with a reference node. Thus, the motion of the right end surface is governed by the motion of the reference node, which is fixed in two translational directions (U_y and U_z) and three rotational directions (R_x , R_y and R_z), while a pull load is applied along the U_x direction.

4.2. Failure criteria of the cohesive elements

Cohesive elements were used to model the debonding crack along the bondline. A bilinear traction-separation law was used to define the

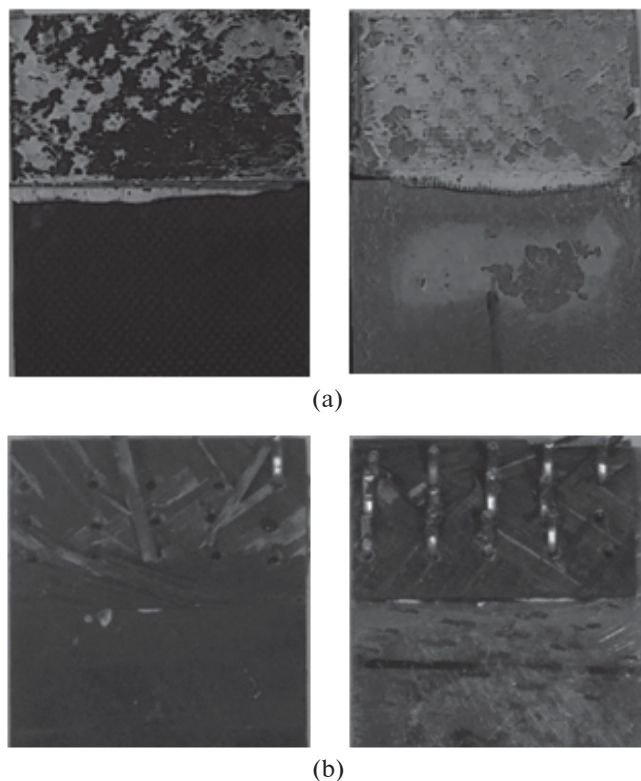


Fig. 4. Failure modes of the joints: (a) Traditional adhesive bonded joints; (b) Proposed joints

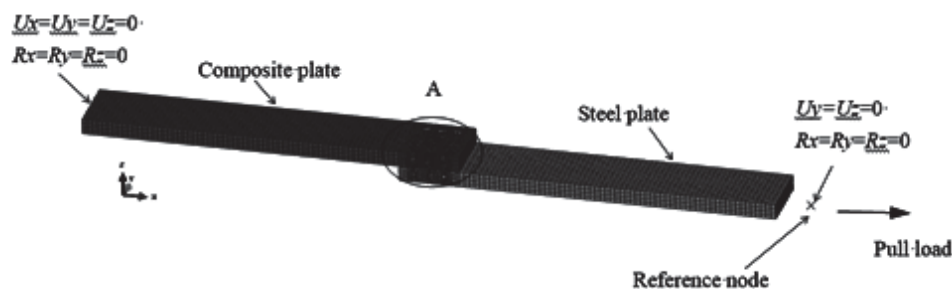


Fig. 5. Finite element model of the proposed joint

constitutive response of cohesive elements. In ABAQUS, the damage factor D (SDEG: Scalar stiffness degradation, $0 \leq D \leq 1$) is introduced to characterize the degree of damage for the cohesive element. The stiffness coefficient K in damage evolution is expressed by

$$K = (1 - D)K_0 \tag{1}$$

where K_0 is the stiffness of complete material. When D equals to 0, it means that the material does not yield or has just begun to yield; when D equals to 1, it means the material has been damaged and the load carrying capacity is lost.

Damage is assumed to initiate when the maximum nominal stress ratio (as defined in the expression below) reaches a value of one. This criterion can be presented as:

$$\max \left(\frac{\langle t_n \rangle}{t_n^0}, \frac{t_s}{t_s^0}, \frac{t_s}{t_t^0} \right) = 1 \tag{2}$$

where, t_n^0 represents the peak value of the nominal stress when the deformation is purely normal to the contact surface, t_s^0 represents the peak value of the nominal stress when the deformation is purely in the first shear direction, and t_t^0 represents the peak value of the nominal stress when the deformation is purely in the second shear direction. The symbol $\langle \rangle$ used in the discussion above represents the Macaulay bracket with the usual interpretation. The Macaulay brackets are used to signify that a pure compressive deformation or stress state does not initiate damage.

$$\langle t_n \rangle = \begin{cases} t_n, & t_n > 0 \\ 0, & t_n \leq 0 \end{cases} \tag{3}$$

The dependence of the fracture energy on the mixed mode can be defined based on a power law fracture criterion. This criterion states that the failure under mixed mode is governed by an interaction law of the energies which cause failure in the single (normal and two shear) mode. It is given by:

$$\frac{G_I}{G_{IC}} + \frac{G_{II}}{G_{IIC}} + \frac{G_{III}}{G_{IIIC}} = 1 \tag{4}$$

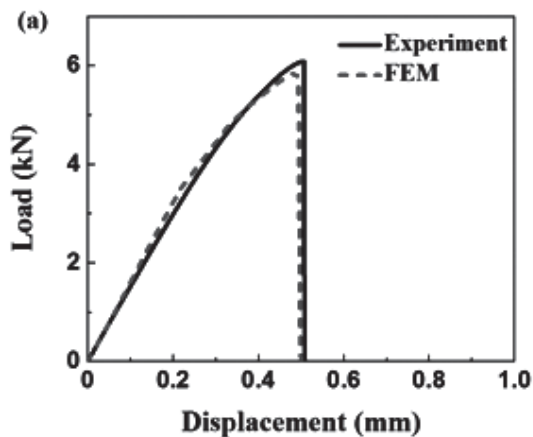
where G_{IC} , G_{IIC} and G_{IIIC} indicate the critical fracture energies required to cause failure in the normal, the

first and the second shear directions, respectively. The displacement at failure (δ^f) is determined by the critical fracture energies GC , which is corresponding to the area under the traction–separation curve.

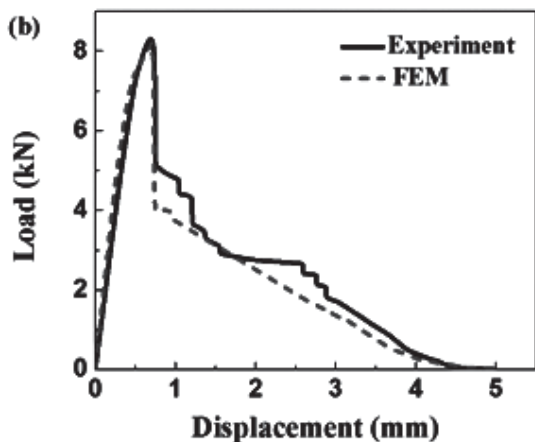
5. Comparison of the test and simulation results

The comparison of the simulated and experimental load-displacement curve of the joint without pins was shown in Fig. 6(a). It is observed from Fig. 6(a) that simulated results of FE model show good agreement with the experimental data, which validates the cohesive finite model for the adhesive joint. The FE model provides an accurate prediction for the joint strength (error < 2.5%). The load-displacement curve remains linear elastic until the yield stress of the metallic plate is reached. The load of adhesive joint increases linearly with the displacement at the beginning, then goes nonlinear with the displacement until reaches its peak.

The numerical and experimental results of load-displacement of the adhesive-multi pin joint are shown



(a)



(b)

Fig. 6. Comparison between numerical and experimental load and displacement curves: (a) Without pins; (b) With pins

in Fig. 6(b). The load increases linearly in the beginning and when it accesses its peak, the adhesive layer begins to break. From this point of view, the load is completely carried by the pin bridging force. The numerical results are in good agreement with the experimental data in whole process. With the increase of displacement, the metallic pin is gradually cut off or pulled out and the carrying capacity of the joint is gradually reduced to zero.

6. Damage tolerance of the composite-metal joint

The strength of the adhesive bonded joint will decrease greatly due to the existence of manufacturing defect and damage in survive. The effect the pins on the adhesive joint with different area of debonding was also studied by test. The specimens with different area of debonding are diagrammatically shown in Fig. 7, in which, the L is the length of debonding of joint. $L = 0$ mm (complete adhesive), $L = 3$ mm, 6 mm, 9 mm and 12 mm (complete disbonding), respectively were compared.

The results are shown in Fig. 8. From Fig. 8, it can be seen that the load-carrying capacity and energy

absorption of the novel joining structures show a trend of decreasing with the increase of disbonding length. Even though the interface layer was completely destroyed, the connection structures still have quite high load carrying capacity. The changes of energy absorption capacity and load carrying capacity were small. When the disbonding length is shorter ($L \leq 3$ mm), the performance of the joint basically does not apparently change.

7. Conclusion

1) The proposed joint method can increase the strength, the failure strain of the metal-composite joints comparing with the traditional adhesive joints, moreover, the joint method can decrease the suddenness of the joint significantly and therefore, improve the damage tolerance performance of the bonded joints.

2) The pins running through the joint plates not only arrest the cracks in the adhesive layer of the bonded joints, also transfer some load.

3) The proposed joint has good damage tolerance performance.

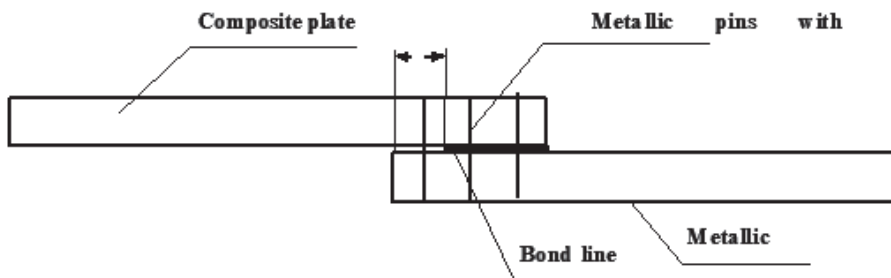


Fig. 7. Adhesive joint with different length of debonding

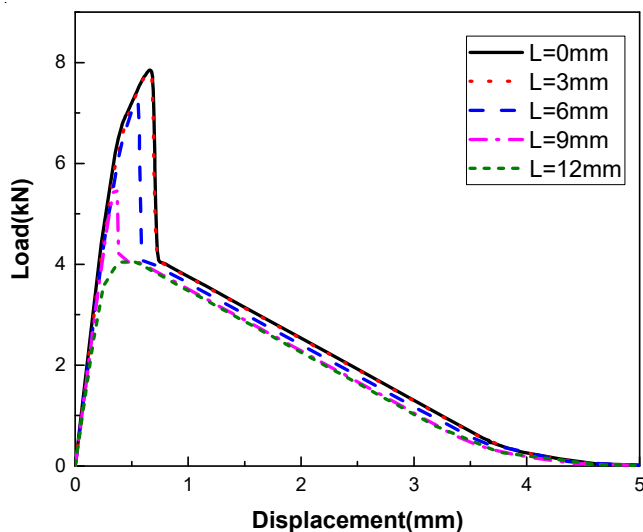


Fig. 8. Load-displacement curves under different debonding length of joint

Acknowledgments

The authors thanks the sponsors and financial support of the National Natural Science Foundation of China (Grant No. U1637105), the Aeronautical Science Foundation of China (2016ZE57009), and the Fundamental Research Funds for the Central Universities (17X100040056).

References

- Zimmermann K., Zenkert D., Siemetzki M. Testing and analysis of ultra thick composites. *Composites Part B: Engineering*, 2010, vol. 41, no. 4, pp. 326-336. DOI: 10.1016/j.compositesb.2009.12.004
- Wu F.Q., Yao W.X. A model of the fatigue life distribution of composite laminates based on their static strength distribution. *Chinese Journal of Aeronautics*, 2008, vol. 21, no. 3, pp. 241-246. DOI: 10.1016/S1000-9361(08)60031-X

3. Löbel T., Holzhüter D., Sinapius M., Hühne C. A hybrid bondline concept for bonded composite joints. *International Journal of Adhesion and Adhesives*, 2016, vol. 68, pp. 229-238. DOI: 10.1016/j.ijadhadh.2016.03.025
4. Yoon T.H., Kim S.J. Refined numerical simulation of three-dimensional riveting in laminated composites. *Journal of Aircraft*, 2011, vol. 48, no. 4, pp. 1434-1443. DOI: 10.2514/1.C031311
5. Restivo G., Marannano G., Isaicu G.A. Three-dimensional strain analysis of single-lap bolted joints in thick composites using fibre-optic gauges and the finite-element method. *The Journal of Strain Analysis for Engineering Design*, 2010, vol. 45, no. 7, pp. 523-534. DOI: 10.1243/03093247JSA599
6. Sen F., Pakdil M., Sayman O., Benli S. Experimental failure analysis of mechanically fastened joints with clearance in composite laminates under preload. *Materials & Design*, 2008, vol. 29, no. 6, pp. 1159-1169.
7. Budhe S., Banea M.D., de Barros S., da Silva L.F.M. An updated review of adhesively bonded joints in composite materials. *International Journal of Adhesion and Adhesives*, 2017, vol. 72, pp. 30-42. DOI: 10.1016/j.ijadhadh.2016.10.010
8. *Advisory circular 20-107B subject: composite aircraft structure* U.S. Department of Transportation – Federal Aviation Administration (FAA), 2010.
9. *AMC 20-29 Annex II to ED Decision 2010/003/R of 19/07/2010*. European Aviation Safety Agency (EASA), 2009.
10. Richard L., Lin K.Y. Analytical and Experimental Studies on Delamination Arrest in Bolted-Bonded Composite Structures. *58th AIAA/ASCE/AHS/ASC Structures, Structural Dynamics, and Materials Conference*. 9 - 13 January 2017, Grapevine, Texas, 2017, pp. 1-12. DOI: 10.2514/6.2016-1502
11. Richard L.I., Liu W., Lin K.Y. Delamination Arrest by Multiple Fasteners in Bonded Composite Structures. *55th AIAA/ASME/ASCE/AHS/ASC Structures, Structural Dynamics, and Materials Conference*, National Harbor, Maryland, 2014, 10 p.
12. Action J.E., Engelstad S.P. Crack Arrestment of Pi-Joined Bonded Composites. *55th AIAA/ASME/ASCE/AHS/ASC Structures, Structural Dynamics, and Materials Conference*, National Harbor, Maryland, 2014, 17 p.
13. Huang J., Rapoff A. J., Haftka R.T. Arresting cracks in bone-like composites. *44th AIAA/ASME/ASCE/AHS Structures, Structural Dynamics, and Materials Conference*, Virginia, 2003, 11 p.
14. Kruse T., Körwien T., Heckner S., Geistbeck M. Bonding of CFRP primary aerospace structures—crackstopping in composite bonded joints under fatigue. *Proceedings of the 20th International Conference on Composite Materials (ICCM/20)*, Copenhagen, 19-24th July 2015, pp. 795-808.
15. Sachse R., Picket A.K., Käß M., Middendorf P. Numerical simulation of fatigue crack growth in the adhesive bondline of hybrid CFRP joints. *Proceedings of the conference on the mechanical response of composites (ECCOMAS)*, Bristol, 2015.
16. Freeman R., Smith F. Comeld: a novel method of composite to metal joining. *Advanced Material Process*, 2005, vol. 163, no. 4, pp. 33-40.